ELSEVIER

Journal of Alloys and Compounds 408–412 (2006) 1173–1176

Journal of ALLOYS AND COMPOUNDS

www.elsevier.com/locate/jallcom

Synthesis and crystal structure of (Ca, R)(Mn, Ti)O_3 (R, rare earth)

Migaku Kobayashi [a,*], Ryouko Katsuraya [a], Syou Kurita [a], Makoto Yamaguchi [b], Hiroshisa Satoh [b], Naoki Kamegashira [b]

[a] *Department of Chemistry and Biochemistry, Numazu College of Technology, 3600 Ooka, Numazu 410-8501, Japan*
[b] *Department of Materials Science, Toyohashi University of Technology, Tempaku-cho, Toyohashi 441-8580, Japan*

Received 30 July 2004; received in revised form 31 October 2004; accepted 15 December 2004
Available online 1 July 2005

Abstract

New compounds of rare earth complex oxides with perovskite structure in a combination of Mn with Ti ions in B-site, $Ca_{0.5}R_{0.5}Mn_{0.5}Ti_{0.5}O_3$ (R = La, Nd, Eu) and $Ca_{0.67}R_{0.33}Mn_{0.33}Ti_{0.67}O_3$ (R = Y, Gd, Dy, Ho, Yb) were synthesized. The powder X-ray diffraction peaks could be indexed as an orthorhombic cell. Rietveld refinement of X-ray diffraction data were carried out based on the space group *Pnma* (No. 62) corresponding to $GdFeO_3$ type perovskite structure. The cell parameters *b*, *c* and cell volume increase with increasing ionic radius of rare earth element. The decrease in ionic radius of rare earth ions in these compounds makes increase distortion from ideal cubic perovskite. Although tendencies of bond distances and bond angles by ionic radius of rare earth element are same in these two kinds of compounds, the change in $Ca_{0.5}R_{0.5}Mn_{0.5}Ti_{0.5}O_3$ is larger than in $Ca_{0.67}R_{0.33}Mn_{0.33}Ti_{0.67}O_3$.

Keywords: Perovskite; Crystal structure; X-ray diffraction; Rare earth manganese oxide

1. Introduction

Rare earth manganese oxides with a substitution of alkaline earth elements have been noted for colossal magnetoresistivity effect (CMR) [1–5]. Rare earth complex oxides including manganese and titanium were studied by several authors [6–8]. Several compounds were prepared for various combinations of La and alkaline earth or Y by Havinga [6], to study a dilution of magnetic interaction between Mn ions via oxygen ion by substitution of Ti ion. It is considered that the tetravalent titanium ion makes the cation–anion–cation overlap integrals weaken in $La_{0.1}Ca_{0.9}Mn_{1-x}Ti_xO_3$ [7]. Furthermore, some compounds were synthesized and refined by the present authors [8]. These compounds have various crystal structures for rare earth in A-site of perovskite structure. For example the crystal structure of $Ba_{0.5}La_{0.5}Mn_{0.5}Ti_{0.5}O_3$, $Sr_{0.5}La_{0.5}Mn_{0.5}Ti_{0.5}O_3$, and $Ca_{0.5}Sm_{0.5}Mn_{0.5}Ti_{0.5}O_3$ are cubic ($Pm\bar{3}m$), rhombohedral ($R3c$) and orthorhombic system (*Pnma*), respectively [8].

In this work syntheses of several compounds with perovskite structure including a combination of manganese and titanium ions were tried to know the existent phases for further study on physical and chemical properties. $Ca_{0.5}R_{0.5}Mn_{0.5}Ti_{0.5}O_3$ (R = La, Nd, Eu), which replaced Sm^{3+} of $Ca_{0.5}Sm_{0.5}Mn_{0.5}Ti_{0.5}O_3$ with La^{3+}, Nd^{3+}, and Eu^{3+} were successfully synthesized to discuss about the influence of rare earth ions to the crystal structure. Although it is a little difficult to form single phases for rare earth elements with decreasing ionic radius after Eu^{3+}, $Ca_{0.67}R_{0.33}Mn_{0.33}Ti_{0.67}O_3$ (R = Y, Gd, Dy, Ho, Yb) were successfully synthesized by increasing Ca^{2+} content in A-site in order to enlarge the size of ions in A-site. These crystal structures were determined by Rietveld analysis of X-ray powder diffraction data and formation of phases is discussed.

2. Experimental

A polycrystalline sample of $Ca_{0.5}R_{0.5}Mn_{0.5}Ti_{0.5}O_3$ (R = La, Nd, Eu) and $Ca_{0.67}R_{0.33}Mn_{0.33}Ti_{0.67}O_3$ (R = Y, Gd, Dy, Ho, Yb) was prepared by the solid-state reaction method.

* Corresponding author. Tel.: +81 55 926 5858; fax: +81 55 926 5858.
E-mail address: m.kobayashi@numazu-ct.ac.jp (M. Kobayashi).

0925-8388/$ – see front matter © 2005 Elsevier B.V. All rights reserved.
doi:10.1016/j.jallcom.2004.12.129

All the starting materials had 99.9% and over purity and were pre-treated to adjust the oxygen stoichiometry [8]. Mixture of R_2O_3, $CaCO_3$, Mn_2O_3, and TiO_2 in appropriate molar ration were pressed into pellets and heated at 1273 K for 3d in a purified Ar flow.

X-ray powder diffraction data of the sample were collected using Cu Kα radiation equipped with a single crystal graphite monochromator. The 2θ range was $20^\circ < 2\theta < 120^\circ$ with increments of 0.04°. The resulting data were analyzed by the Rietveld method using the RIETAN program [9,10]. The initial setting values of the lattice parameters for the Rietveld analysis were used for the values determined from a least square method.

3. Results and discussion

The powder X-ray diffraction pattern of $Ca_{0.5}R_{0.5}Mn_{0.5}Ti_{0.5}O_3$ (R = La, Nd, Eu) and $Ca_{0.67}R_{0.33}Mn_{0.33}Ti_{0.67}O_3$ (R = Y, Gd, Dy, Ho, Yb) were shown in Figs. 1 and 2, respectively. All the peaks on X-ray diffraction patterns could be indexed as an orthorhombic phase corresponding to $GdFeO_3$ type perovskite structure. It seems that the powder X-ray diffraction pattern of $Ca_{0.5}La_{0.5}Mn_{0.5}Ti_{0.5}O_3$ might be different from other patterns. But it sees carefully, the peak of 200, 121, and 210 overlap and it is visible to one. In a similar way, the peaks of 101, 220, 202, and 123 are seen one peak with another surrounding peaks, respectively.

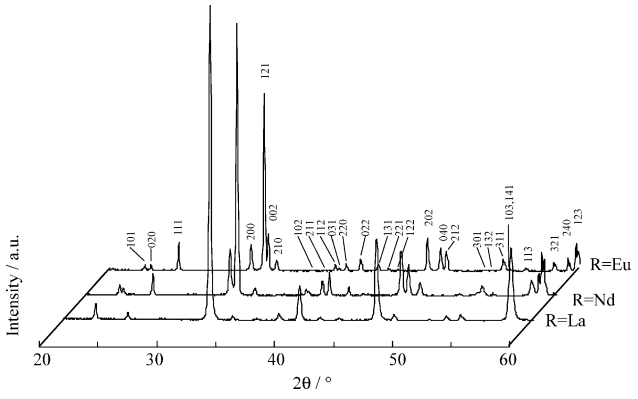

Fig. 1. Powder X-ray diffraction patterns of $Ca_{0.5}R_{0.5}Mn_{0.5}Ti_{0.5}O_3$. The observable peaks of $Ca_{0.5}Eu_{0.5}Mn_{0.5}Ti_{0.5}O_3$ were indicated by mirror index as orthorhombic system.

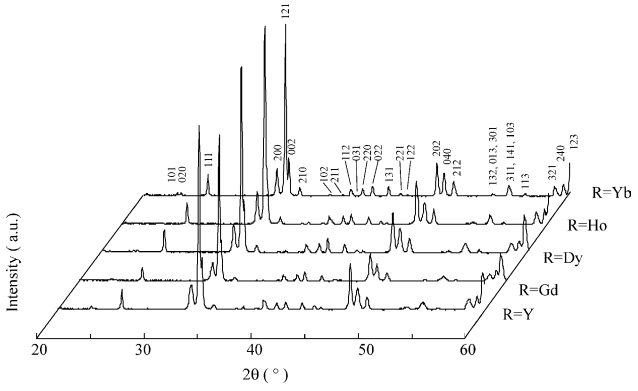

Fig. 2. Powder X-ray diffraction patterns of $Ca_{0.67}R_{0.33}Mn_{0.33}Ti_{0.67}O_3$. The observable peaks of $Ca_{0.5}Yb_{0.5}Mn_{0.5}Ti_{0.5}O_3$ were indicated by mirror index as orthorhombic system.

Table 1
Crystallographic data and fractional atomic coordinates of $Ca_{0.5}R_{0.5}Mn_{0.5}Ti_{0.5}O_3$

	R = La	R = Nd	R = Eu
a (nm)	0.55128 (2)	0.55471 (2)	0.55849 (1)
b (nm)	0.77615 (4)	0.76632 (3)	0.75553 (2)
c (nm)	0.54871 (2)	0.54309 (2)	0.53461 (1)
R_{wp} (%)	9.52	13.50	13.68
S	1.41	1.89	1.53
$x_{(Ca,R)}$	0.0272 (4)	0.0441 (6)	0.0613 (5)
$z_{(Ca,R)}$	0.005 (1)	−0.009 (1)	−0.0131 (9)
x_{O1}	−0.0115 (3)	−0.023 (4)	−0.032 (3)
z_{O1}	0.575 (7)	0.591 (7)	0.399 (4)
x_{O2}	0.213 (3)	0.207 (3)	0.299 (3)
y_{O2}	−0.033 (3)	−0.043 (3)	0.046 (2)
z_{O2}	0.785(3)	0.784 (3)	0.708 (3)
$B_{(Ca,R)}$ (nm^2)	0.0076 (5)	0.0063 (9)	0.0087 (8)
$B_{(Mn,Ti)}$ (nm^2)	0.008 (6)	0.005 (1)	0.005 (1)
B_{O1} (nm^2)	0.014 (8)	0.021 (8)	0.012 (5)
B_{O2} (nm^2)	0.007 (4)	0.003 (5)	0.006 (4)

Space group *Pnma*; (Ca, R) and O1 in 4*c*(x, 1/4, z), (Mn, Ti) in 4*a*(0, 1/2, 1/2), and O2 in 8*d*(x, y, z).

Rietveld refinement of X-ray diffraction data was carried out by RIETAN program based on the orthorhombic cell of dimensions with $\sqrt{2}a_c \times 2a_c \times \sqrt{2}a_c$ in the space group *Pnma* (no. 62), where a_c is ideal cubic perovskite cell parameter. These crystallographic data are listed Tables 1 and 2 and the observed and calculated profiles of $La_{0.5}Ca_{0.5}Mn_{0.5}Ti_{0.5}O_3$ are shown in Fig. 3. These profiles are in agreement with the *Pnma* model with a little higher value of R_{wp} (weighted pattern R-factor) and a coefficient S (goodness of fits). The cell parameters b and c increase with increasing ionic radius of rare earth element. While the cell parameter a decrease with increasing ionic radius of rare earth element in $Ca_{0.5}R_{0.5}Mn_{0.5}Ti_{0.5}O_3$, and only little changes

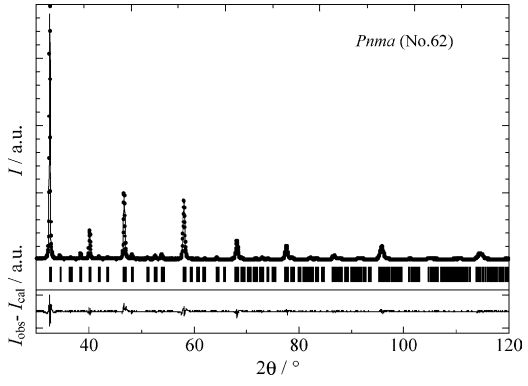

Fig. 3. The observed and calculated profiles of $Ca_{0.5}La_{0.5}Mn_{0.5}Ti_{0.5}O_3$. Experimantal points are shown by dots and the calculated profile by a solid line. The small bars indicate the angular positions of the allowed Bragg reflections.

Table 2
Crystallographic data and fractional atomic coordinates of $Ca_{0.67}R_{0.33}Mn_{0.33}Ti_{0.67}O_3$

	R = Y	R = Gd	R = Dy	R = Ho	R = Yb
a (nm)	0.55224 (4)	0.55189 (4)	0.55230 (3)	0.55242 (2)	0.55171 (2)
b (nm)	0.75893 (5)	0.76183 (5)	0.75960 (4)	0.75900 (3)	0.75726 (3)
c (nm)	0.53576 (3)	0.53831 (3)	0.53663 (3)	0.53569 (2)	0.53382 (2)
R_{wp} (%)	14.18	15.91	13.33	12.39	11.37
S	1.72	1.74	1.67	1.49	1.29
$x_{(Ca,R)}$	0.0538 (3)	0.0496 (4)	0.0539 (3)	0.0545 (3)	0.0582 (2)
$z_{(Ca,R)}$	−0.0123 (5)	−0.0102 (7)	−0.0112 (5)	−0.0127 (5)	−0.0132 (4)
x_{O1}	0.470 (1)	0.472 (3)	0.472 (2)	0.470 (1)	0.469 (2)
z_{O1}	0.0944 (2)	0.097 (3)	0.096 (2)	0.099 (2)	0.105 (2)
x_{O2}	0.295 (1)	0.209 (2)	0.204 (1)	0.295 (1)	0.199 (1)
y_{O2}	0.0444 (8)	0.544 (1)	0.539 (1)	0.0439 (9)	0.544 (1)
z_{O2}	−0.294 (1)	0.215 (2)	0.208 (1)	−0.292 (1)	0.204 (1)
$B_{(Ca,R)}$ (nm^2)	0.0049 (6)	0.0030 (7)	0.0031 (5)	0.0058 (5)	0.0073 (4)
$B_{(Mn,Ti)}$ (nm^2)	0.0028 (6)	0.0037 (9)	0.0022 (6)	0.0023 (6)	0.0029 (5)
B_{O1} (nm^2)	0.010 (2)	0.003 (3)	0.002 (2)	0.012 (2)	0.011 (2)
B_{O2} (nm^2)	0.003 (1)	0.0 (2)	0.001 (2)	0.002 (2)	0.007 (2)

Space group *Pnma*; (Ca, R) and O1 in 4*c*(*x*, 1/4, *z*), (Mn, Ti) in 4*a*(0, 0, 1/2), and O2 in 8*d*(*x*, *y*, *z*).

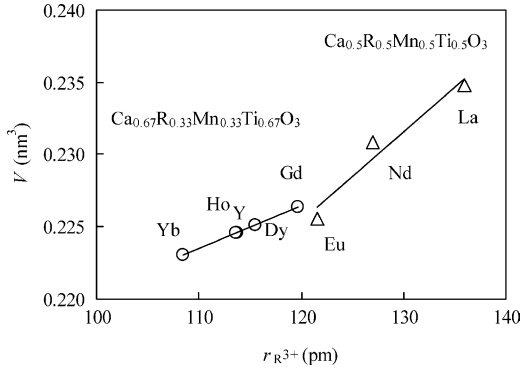

Fig. 4. Cell volume of $Ca_{0.5}R_{0.5}Mn_{0.5}Ti_{0.5}O_3$, and $Ca_{0.67}R_{0.33}Mn_{0.33}Ti_{0.67}O_3$.

with ionic radius changed in $Ca_{0.67}R_{0.33}Mn_{0.33}Ti_{0.67}O_3$. Although the values of cell parameter change with tendencies that were described above, the cell volume increases linearly with increasing ionic radius of rare earth element as is shown in Fig. 4. The change of cell volume in $Ca_{0.5}R_{0.5}Mn_{0.5}Ti_{0.5}O_3$ is larger than in $Ca_{0.67}R_{0.33}Mn_{0.33}Ti_{0.67}O_3$.

The octahedron around trivalent manganese and tetravalent titanium ions of these compounds were distorted. For $Ca_{0.67}Yb_{0.33}Mn_{0.33}Ti_{0.67}O_3$, distorted octahedron and overview of structure were shown in Figs. 5 and 6, respectively. The mean distance of (Mn,Ti)-O is about 198 pm and is comparable with the distance of 200 pm calculated weighted average from the ionic radii of Shannon and Prewitt [11]. The mean tilting angle is approximately 15° toward each zigzag connection.

There were eight oxygen ions with shorter distances and four with longer distances among the twelve oxygen ions surrounding the A-site ion. The average bond distances between A-site ion and oxygen ions were shown in Fig. 7. The distances increase with increasing ionic radius

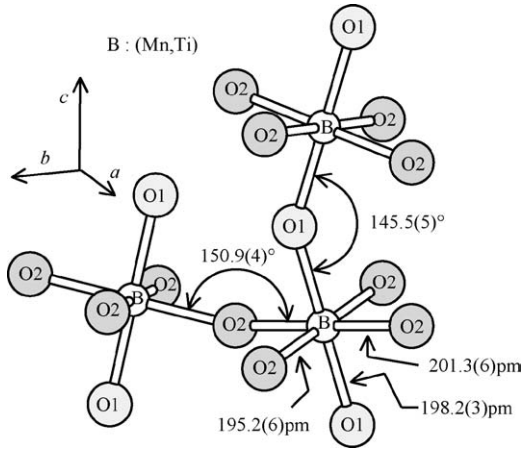

Fig. 5. Distorted octahedron of $Ca_{0.67}Yb_{0.33}Mn_{0.33}Ti_{0.67}O_3$ around Mn and Ti ions.

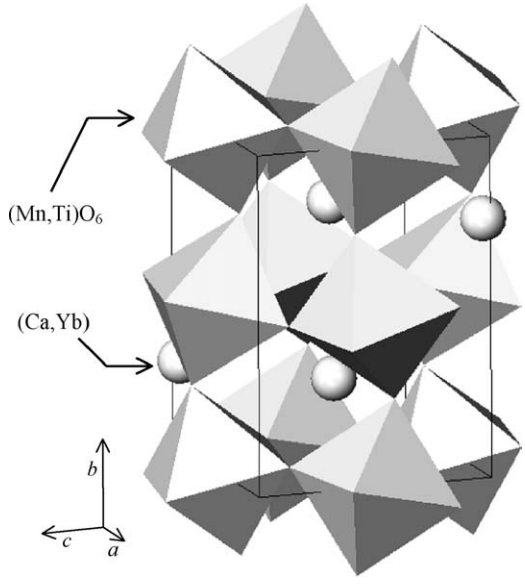

Fig. 6. Overview of the structure of $Ca_{0.67}Yb_{0.33}Mn_{0.33}Ti_{0.67}O_3$.

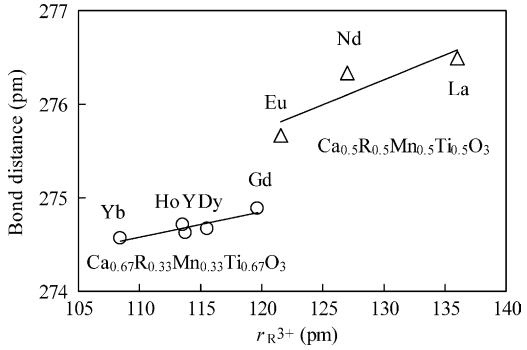

Fig. 7. Bond distance of $Ca_{0.5}R_{0.5}Mn_{0.5}Ti_{0.5}O_3$, and $Ca_{0.67}R_{0.33}Mn_{0.33}Ti_{0.67}O_3$ around (Ca, R) and O ions. An average value of each bond is used.

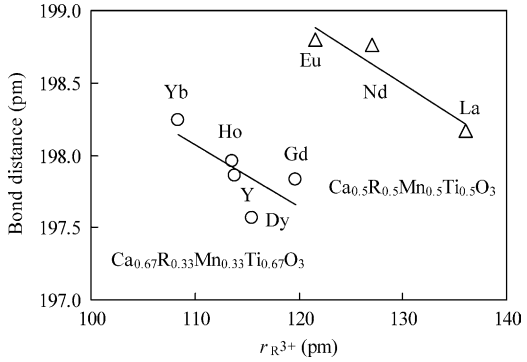

Fig. 8. Bond distance of $Ca_{0.5}R_{0.5}Mn_{0.5}Ti_{0.5}O_3$, and $Ca_{0.67}R_{0.33}Mn_{0.33}Ti_{0.67}O_3$ around (Mn, Ti) and O ions. An average value of each bond is used.

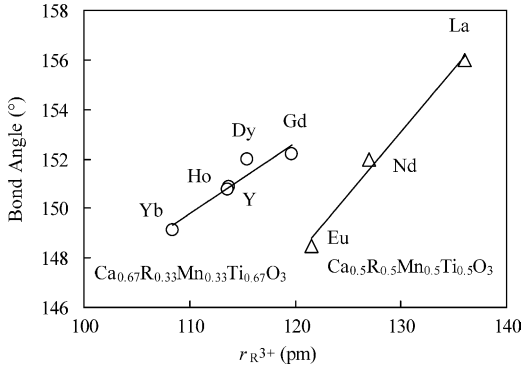

Fig. 9. The angles between oxygen octahedrons surrounding the Mn^{3+} and Ti^{4+} in $Ca_{0.5}R_{0.5}Mn_{0.5}Ti_{0.5}O_3$, and $Ca_{0.67}R_{0.33}Mn_{0.33}Ti_{0.67}O_3$. An average value of each bond is used.

of rare earth element. The oxygen octahedra around the B-site are only slightly distorted and tilted against each other like zigzag chains in each direction. The average bond distances between B-site ion and oxygen ions were shown in Fig. 8. The averages of bond angles between oxygen octahedrons surrounding the trivalent manganese ion and tetravalent titanium ions were shown in Fig. 9. Although it seems the values of distance in $Ca_{0.67}Dy_{0.33}Mn_{0.33}Ti_{0.67}O_3$, and $Ca_{0.67}Gd_{0.33}Mn_{0.33}Ti_{0.67}O_3$ were shifted from an approximation straight line slightly, with the increase in ionic radius of rare earth, the distances decrease and a degree between oxygen octahedral by zigzag arrangement becomes smaller. It seems that this phenomenon is related to tendency about the distances between A-site and oxygen ions.

From above discussion, the decrease in ionic radius of rare earth ions in these compounds makes increase distortion from ideal cubic perovskite. Although tendencies of bond distances and bond angles by ionic radius of rare earth element are same in these two kinds of compounds, the change in $Ca_{0.5}R_{0.5}Mn_{0.5}Ti_{0.5}O_3$ is larger than in $Ca_{0.67}R_{0.33}Mn_{0.33}Ti_{0.67}O_3$. Since the composition ratio of rare earth in A-site differ between $Ca_{0.5}R_{0.5}Mn_{0.5}Ti_{0.5}O_3$, and $Ca_{0.67}R_{0.33}Mn_{0.33}Ti_{0.67}O_3$, this difference is reasonable.

Acknowledgement

This work was supported by the grant-in-aid for Scientific Research (B) (No. 13450259) by the Japan Society for the Promotion of Science.

References

[1] A. Urushibara, Y. Morimoto, T. Arima, A. Asamitsu, G. Kido, Y. Tokura, Phys. Rev. B 51 (1995) 14103.
[2] R. Mahesh, R. Mahendiran, A.K. Raychaudhuri, C.N.R. Rao, J. Solid State Chem. 120 (1995) 204.
[3] H. Huhtinen, R. Laiho, K.G. Lisunov, V.N. Stamov, V.S. Zakhvalinskii, J. Magn. Magn. Mater. 238 (2002) 160.
[4] L.Q. Zheng, Q.F. Fang, Phys. Stat. Sol., A 185 (2001) 267.
[5] W.H. McCarroll, K.V. Ramanujachary, D. Ian, M. Fawvett, Greenblatt, J. Solid State Chem. 145 (1999) 88.
[6] E.E. Havinga, Philups Res. 21 (1966) 432.
[7] H. Taguchi, M. Sonoda, M. Nagao, J. Solid State Chem. 26 (1996) 235.
[8] M. Kobayashi, M. Yamaguchi, N. Kamegashira, Proceedings of the International Symposium on Designing Processing and Properties of Advanced Engineering Materials, 1997, p. 505.
[9] F. Izumi, J. Crystallogr. Jpn. 27 (1985) 23.
[10] F. Izumi, J. Mineral. Soc., Jpn. 17 (1985) 37.
[11] R.D. Shannon, C.T. Prewitt, Acta Crystallogr. B 25 (1969) 925.